Int. J. Electrochem. Sci., 13 **(2018)** 10527 – 10538, doi: 10.20964/2018.11.48

International Journal of
ELECTROCHEMICAL
SCIENCE
www.electrochemsci.org

Synergistic Effect of AC and Cl^- on Stress Corrosion Cracking Behavior of X80 Pipeline Steel in Alkaline Environment

Min Zhu[*], *Yongfeng Yuan, Simin Yin, Shaoyi Guo*

School of Mechanical Engineering & Automation, Zhejiang Sci-Tech University, Hangzhou 310018, PR China
[*]E-mail: zmii666@126.com

Received: 22 June 2018 / *Accepted:* 16 August 2018 / *Published:* 1 October 2018

The effect of AC and Cl^- on stress corrosion cracking behavior of X80 pipeline steel was investigated in alkaline solution using slow strain rate tensile (SSRT) tests and polarization curves. The results show that AC and Cl^- generate the synergistic effect, causing a further increase in the SCC susceptibility of X80 pipeline steel. And the fracture surface shows a significant characteristic of brittle fracture. The addition of Cl^- increases the SCC susceptibility of steels with or without AC interference, but the SCC mechanism of steels with or without Cl^- is not changed. When AC current is absent, the SCC mechanism of the steel in 0.2M Cl^- containing alkaline solution is anodic dissolution. In contrast, under AC application, the mechanism is attributed to the combination of anodic dissolution and hydrogen embrittlement.

Keywords: synergistic effect; AC and Cl^-; stress corrosion cracking; pipeline; brittle fracture

1. INTRODUCTION

It is generally known that chloride ion (Cl^-) is a kind of aggressive anion, which could damage the surface passive film and facilitate the occurrence of localized corrosion of carbon steel [1]. Pitting corrosion has often been observed on pipeline steels due to AC interference [2-4]. Movley [5] thought that AC could play a similar role to chloride ions in inducing the pitting corrosion. Our previous research found that AC interference could generate a significant destructive influence to the passive film formed on X80 steel, accelerate the occurrence of serious pitting corrosion, and greatly increase the SCC susceptibility of the steel in carbonate/bicarbonate solution [6-7]. Our latest research has indicated that AC and Cl^- could generate synergistic effect on the corrosion behavior of X80 pipeline steel in alkaline environment, which greatly enhances the corrosion rate of the steel and its corrosion

form becomes more localized [8].

Stress corrosion cracking (SCC) is one of the main corrosion failure forms of pipeline. It is well known that pitting corrosion is one of the important sources of initiation of cracks [9]. Whether AC and Cl^- could generate the synergistic effect to further enhance the SCC susceptibility of pipeline steel, and accelerate the occurrence of SCC failure? This is a very valuable research topic. However, there has been no related reference reported now.

Therefore, in this work, stress corrosion cracking behavior of X80 pipeline steel with AC application was studied in chloride-containing alkaline solution using slow strain rate tensile (SSRT) tests and polarization curves.

2. EXPERIMENTAL

2.1 Material and solution

API X80 pipeline steel was used as the experimental material. The chemical composition of the steel is (wt%): C 0.070,Si 0.216, Mn 1.80, P 0.0137,S 0.0009,Mo 0.182,Cr 0.266,Cu 0.221, Ni 0.168, Nb 0.105, Al 0.026, Ti 0.013, V 0.001, N 0.003 and Fe balance. In the lab, Na_2CO_3/$NaHCO_3$ simulated solution [10] was usually adopted to investigate the stress corrosion cracking (SCC) behavior of pipeline steel buried in alkaline environment. In this work, 0.5M Na_2CO_3+1M $NaHCO_3$ was used to study the SCC behavior of the steel under AC interference. The pH of the solution was about 9.32. The concentration of 0.2 M Cl^- added to the carbonate/bicarbonate solution, which was used to examine the influence of chloride ion on the SCC behavior of the steel interfered by superimposed AC current.

2.2 SSRT test

SCC behavior of the steel in chlorine containing alkaline solution under various AC current densities was studied by SSRT test. The test was carried out via a WDML-30KN Materials Test System. The tensile specimens were prepared in accordance with GB/T 15970 specification [11]. Before the test, the test part of the specimen was polished to 2000 grit emery paper, followed by degreasing with acetone, then rinsed with deionized water, subsequently dried in air. Previous to SSRT test, the specimen was soaked in the solution for 24 h. AC current and DC potential were simultaneously imposed to the specimen through SSRT test. The applied DC potential of -580 mV (vs. SCE) was in the middle of transition region in polarization curve, which could cause IGSCC [12]. The polarized potential was applied to the specimen via a PS-12 potentiostat and a three-electrode cell system, where the tensile specimen was used as the working electrode, a platinum sheet as counter electrode and a saturated calomel electrode (SCE) as reference electrode. Sine wave AC current of 50 Hz with different current densities (0, 30, 50 A/m^2) was imposed to the tensile specimen during the entire SSRT test. The test was performed at room temperature (~22℃) with a strain rate of 1×10^{-6} s^{-1}. To investigate the SCC susceptibility of X80 steel in chlorine containing alkaline solution, sensitivity parameters including reduction-in-area (I_ψ) and elongation-loss rate (I_δ) were calculated [6]. After

SSRT tests, the fracture surfaces of X80 steels were observed using scanning electron microscopy (SEM).

2.3 Polarization curve

For the polarization curves measurement, the specimens were the same as those used in SSRT test, and the schematic diagram of the experimental set-up for AC corrosion is in agreement with the references [6-7]. The steel sample was coated with an epoxy, leaving an exposure area of 1cm^2 as the working surface. The polarization curve test was performed through PARSTAT2273 electrochemical workstation via a three-electrode cell system, where the tensile specimen was used as working electrode, a saturated calomel electrode(SCE) as reference electrode, and a platinum sheet as counter electrode. AC sinusoidal signal was provided by an AT1645-3 function generator. Various AC current densities (0, 30, 50 A/m^2) with 50 Hz in frequency were imposed to the working electrode and graphite electrode. An inductor was adopted to prevent AC interference to electrochemical workstation, while a capacitor was added to avoid the direct current entering the AC mesh. The root-mean-square value of AC current density was measured by a clamp meter. Prior to testing, the tensile specimen was stretched to maximum load through a WDML-30KN Materials Test System at a strain rate of 1×10^{-5} s^{-1}, i.e., tensile strength (the corresponding strain is 15%), and then stopped stretching. The specimen was maintained stationary for 2 h in chloride-containing alkaline solution to reach a steady state. Potentiodynamic polarization curves were measured in the potential range from -1.0 V (vs. SCE) to 1.1 V (vs. SCE) with a potential scanning rate of 0.5 mV/s.

3. RESULTS

3.1 SSRT test

Fig.1 shows the SCC susceptibility of X80 steel in 0.2M Cl^- containing alkaline solution at various AC current densities. It is shown that both I_δ and I_Ψ of steel specimens under AC interference are much greater than that at the absence of AC, and the values of two parameters enhance as the increasing of AC current density. Especially, a more obvious increase can be seen for I_Ψ. The value of I_Ψ is almost up to 60 % at a current density of 50 A/m^2. This demonstrates that AC current enhances the SCC susceptibility of the steel, and the increased AC current density improves the susceptibility. The values of I_Ψ of specimens under AC application are both greater than 51 %, even at 30 A/m^2, which demonstrates that the pipeline steel with AC application has high SCC susceptibility. Further observation reveals that the addition of Cl^- further increases ductility-loss parameters (I_δ and I_Ψ), which indicates that Cl^- facilitates the SCC process, and enhances the SCC susceptibility of the steel.

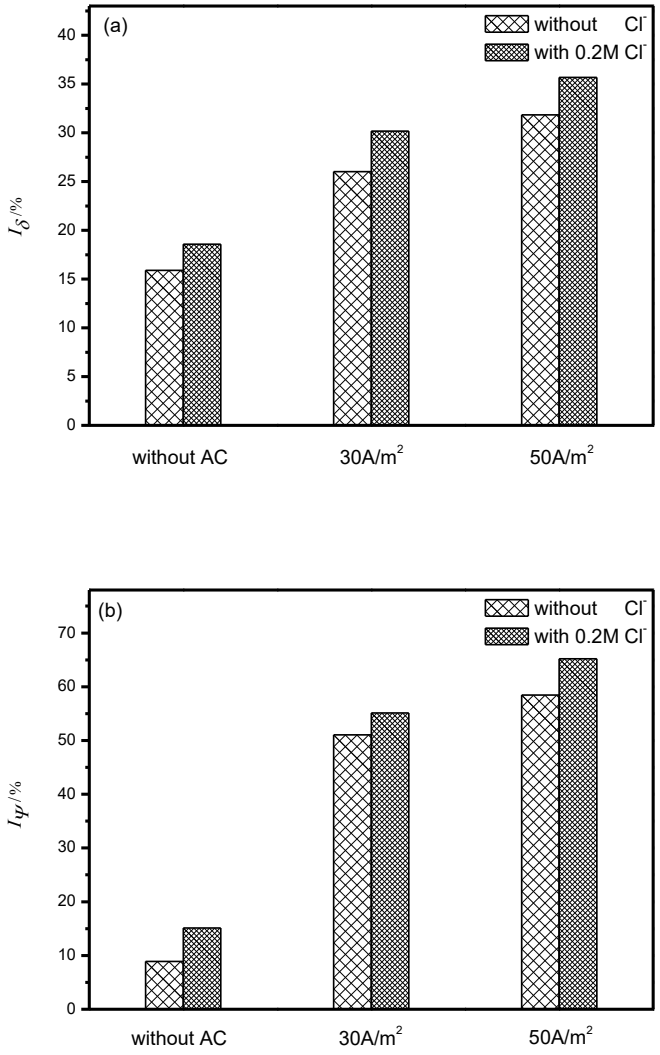

Figure 1. SCC susceptibility of X80 steel in 0.2M Cl^- containing alkaline solution at various AC current densities: (a) elongation-loss rate (I_δ) and (b) reduction-in-area loss rate (I_Ψ)

Fig.2 shows the fractographs of X80 steel in 0.2M Cl^- containing alkaline solution at various AC current densities. As seen in Fig.2a, the fractographs of specimen without AC application exhibits the feature of obvious necking phenomenon, demonstrating that the fracture mode has a feature of ductile fracture. Fig.2b reveals that, the necking degree of fracture surface of the steel decreases with the addition of Cl^- to the solution. And a visible difference in fracture morphologies between the specimens with or without AC interference can be observed. With the increase of AC current density, the necking degree in fractures of the steel specimens obviously reduces and the characteristics of brittle fracture increases (Fig.2c and 2e). When adding Cl^- to the solution, the fracture morphologies of the steel at various AC current densities exhibits very flat macroscopic fracture, and very slight necking phenomenon, which presents an evident characteristic of brittle fracture (Fig.2d and 2f). Combined with the ductility-loss parameters in Fig.1, this suggests that AC and Cl^- produce the synergistic effect, causing a great increase in the SCC susceptibility of X80 pipeline steel. Compared

with the fracture feature of the steel without AC application, the difference in the fractographs means that the SCC mechanism of pipeline steel under AC interference in carbonate/bicarbonate solution may be changed.

The fractographs of specimens with superimposed AC are analogous to that under the effect of hydrogen embrittlement. Moreover, large values of I_Ψ and I_δ (Fig.1) as well as the apparent characteristics of brittle fracture (Fig.2), also suggesting that there is existence of hydrogen embrittlement.

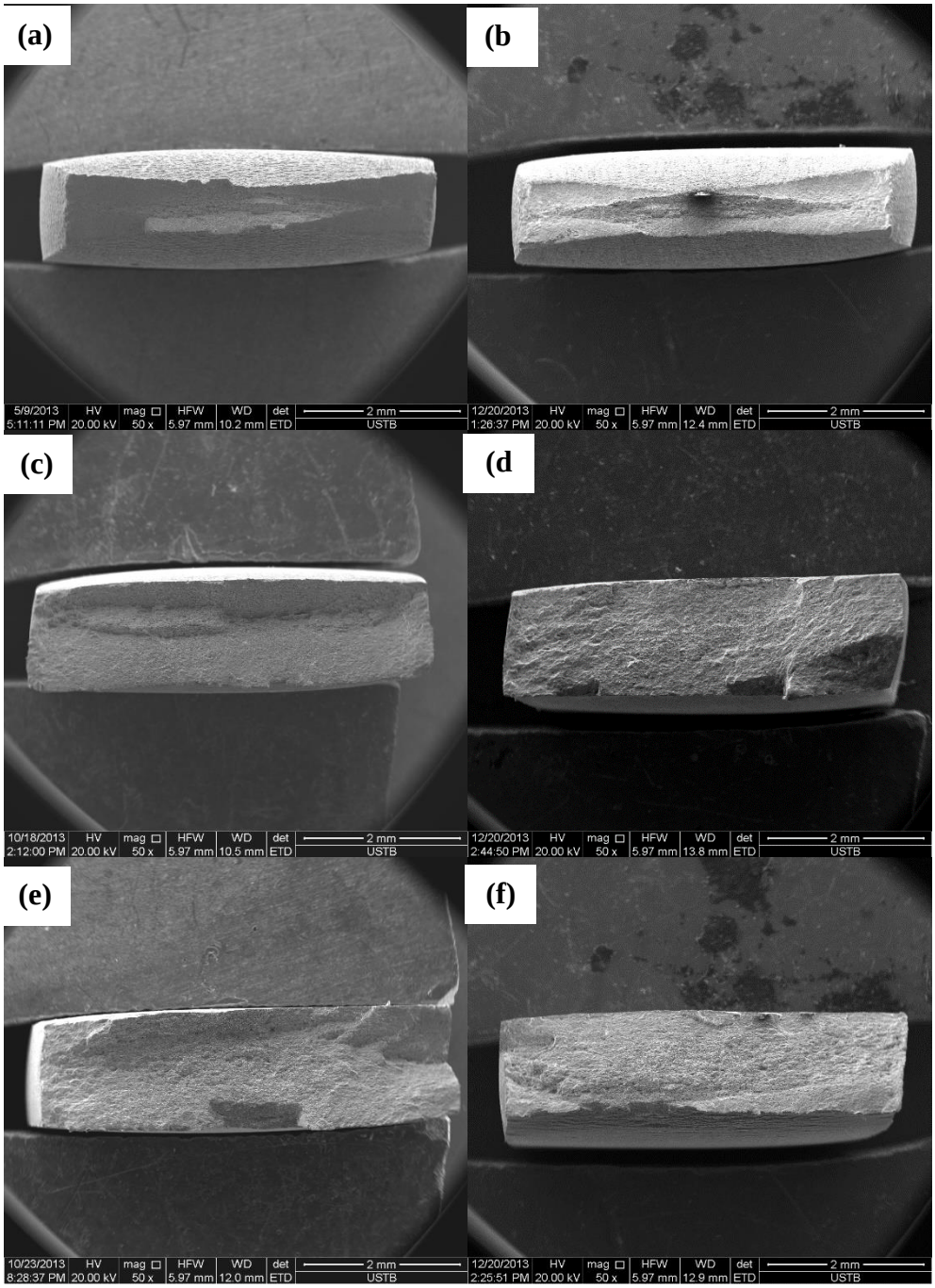

Figure 2. Fractographs of X80 steel in 0.2M Cl^- containing alkaline solution under various AC current densities: (a) 0 A/m^2, (b) 0 A/m^2(with Cl^-), (c) 30 A/m^2, (d) 30 A/m^2(with Cl^-), (e) 50 A/m^2 , (f) 50 A/m^2(with Cl^-)

Fig.3 shows the morphology of the side near fracture surface of X80 steel in 0.2M Cl^- containing alkaline solution under various AC current densities. It clearly reveals that there are significant differences in the morphologies of the side near fracture surface of specimens with or without AC current.

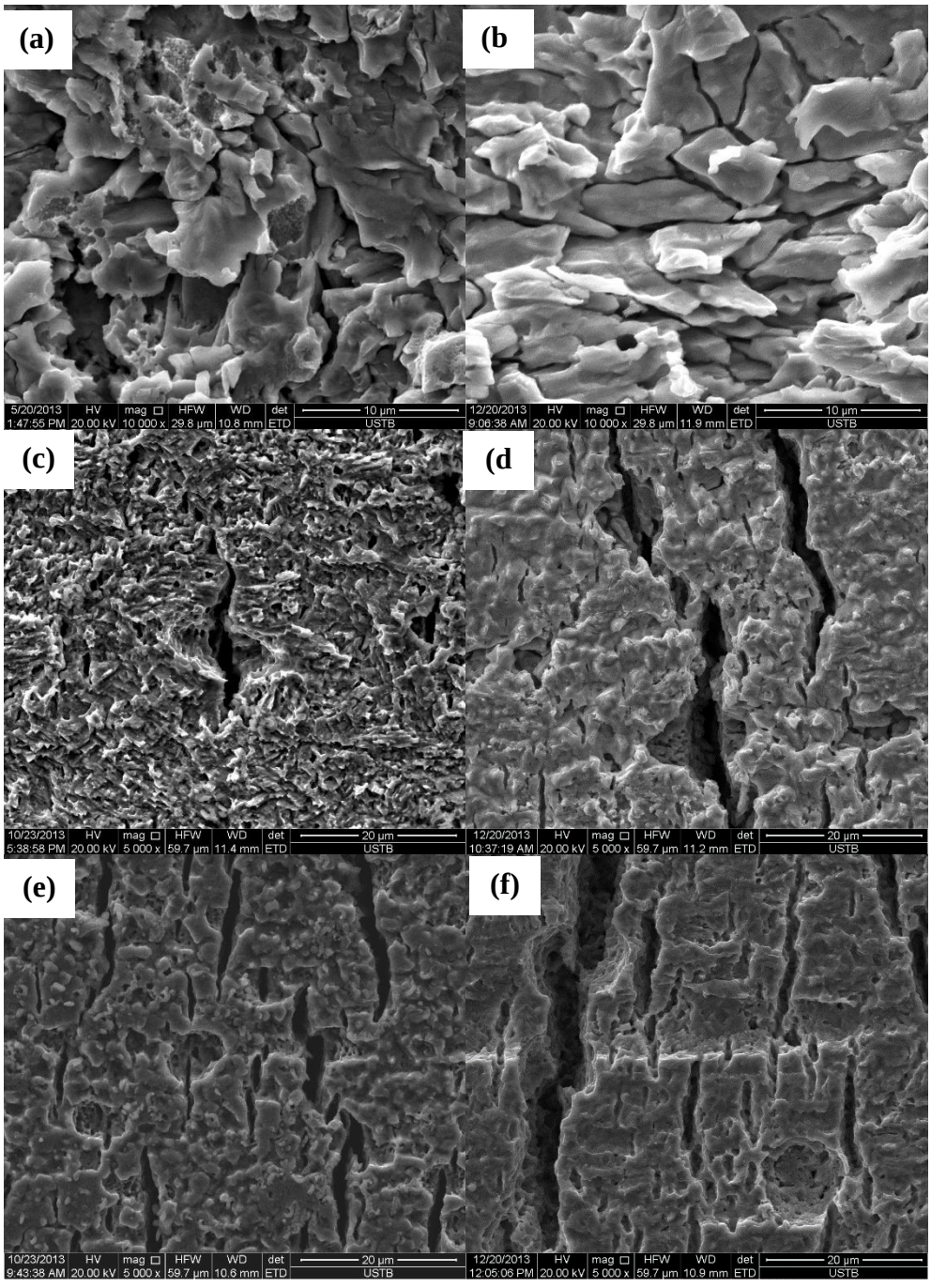

Figure 3. Morphology of the side near fracture surface of X80 steel in 0.2M Cl^- containing alkaline solution under various AC current densities : (a) 0 A/m^2, (b) 0 A/m^2(with Cl^-), (c) 30 A/m^2, (d) 30 A/m^2(with Cl^-), (e) 50 A/m^2 , (f) 50 A/m^2(with Cl^-)

Without the presence of AC current (Fig.3a and 3b), there are some narrow and flexural cracks, and the morphologies show the classical feature of intergranular crack propagation. In addition, no

apparent pitting corrosion is observed in the side near fracture surface, which indicates that the propagation mode is no associated with pits. However, there are the more intensive cracks existing in the fracture of steels with AC application, and the cracks propagation is almost linear, which are identical to the characteristics of the typical transgranular fracture of pipeline [13-14]. Moreover, some short cracks are connected into a long continuous one, which indicates that the resistance of crack propagation is relatively small, and the steel with AC interference has a higher SCC susceptibility.

Fig.3c and 3e also exhibit that some cracks are initiated from the bottom of pits induced by AC interference, which demonstrates that imposed AC can facilitate crack initiation and propagation at some extent. It is clearly seen from Fig.3c-f, an apparent phenomenon of the grain separation can be observed, indicating that the SCC behavior of the steel under AC interference is affected by anodic dissolution. In addition, the propagation path of wide and deep cracks is straight, which is analogous to that of transgranular crack. This demonstrates that hydrogen embrittlement has a significant impact on the SCC behavior. Besides, the SCC cracks become wider and longer (Fig.3d and 3f), demonstrating that the addition of Cl^- further enhances the SCC susceptibility of the steel. The obvious difference in the crack morphologies further demonstrates that the SCC mechanism of X80 steel with or without AC current is different.

Fig.4 shows the cross-sectional fractographs of X80 steel in 0.2M Cl^- containing alkaline solution at various AC current densities. At the absence of AC application (Fig.4a and 4b), the crack propagation mode is an apparent intergranular.

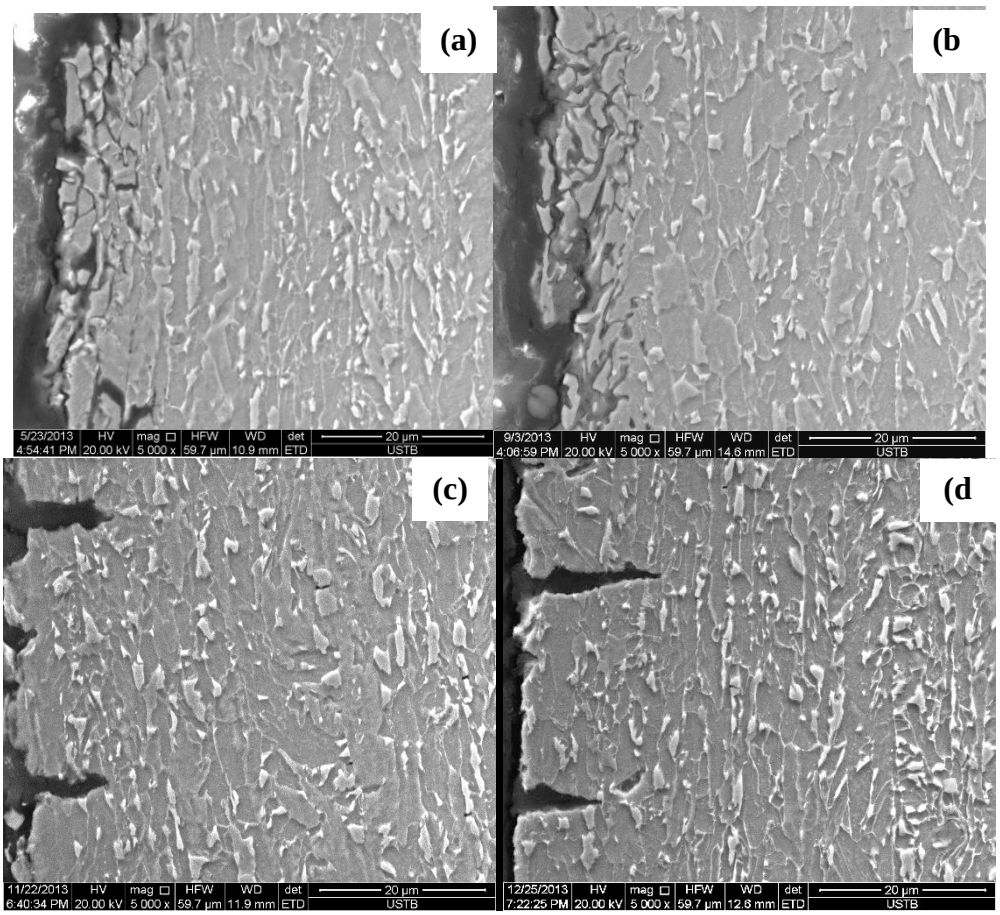

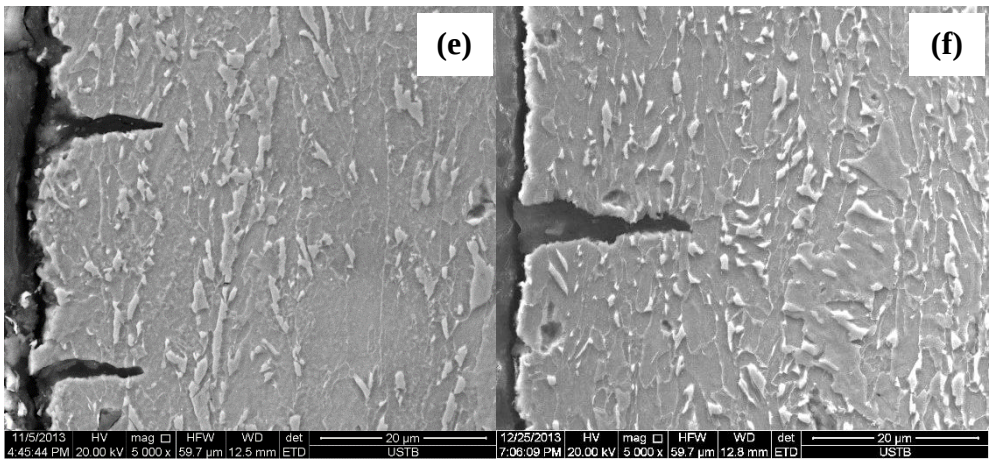

Figure 4. Cross-sectional fractographs of X80 steel in 0.2M Cl^- containing alkaline solution under various AC current densities: (a) 0 A/m^2, (b) 0 A/m^2(with Cl^-), (c) 30 A/m^2, (d) 30 A/m^2(with Cl^-), (e) 50 A/m^2 , (f) 50 A/m^2(with Cl^-)

Under AC application, the crack propagation is a classical transgranular. By comparison, the crack propagation mode of steels with or without AC is significantly different. Further observation indicates that the depth of the crack slightly increases due to the addition of Cl^-.

Based on the above analysis, without AC application, the fracture characteristic and crack propagation mode of steels (with or without Cl^-) are similar to that of the classical IGSCC, which indicate that the SCC mechanism is anodic dissolution [15-19]. It is different that the fracture feature of sample tested under AC is accord with that of TGSCC fracture [20-21]. Combined with the above results, it is concluded that the SCC behavior of pipeline steel with AC interference is controlled by anodic dissolution and hydrogen embrittlement [7,22-23]. Moreover, the addition of Cl^- involves in the SCC process, and increases the SCC susceptibility. However, the SCC mechanism of steels with or without Cl^- is not changed.

3.2 Polarization curve

Fig.5 shows the polarization curves of X80 steel under the condition of some certain strain in 0.2M Cl^- containing solution at various AC current densities. The fitting corrosion parameters are listed in Table.1 and Table.2. With increasing AC current density, the passive region significantly narrows, the critical pitting potential shifts negatively (Table.1) and the passive current density increases (Table.2). This indicates that AC degrades the passivity of the steel. Without the addition of Cl^-, the passivity of the tensile specimens under some certain strain at various AC current densities degrades severely. Because the procreant strain increases the active points on the surface of the specimen and the electrochemical reaction is facilitated. Under the same strain (15%), the passive current density increases due to the addition of 0.2 M Cl^-, and the critical pitting potential shifts negatively.

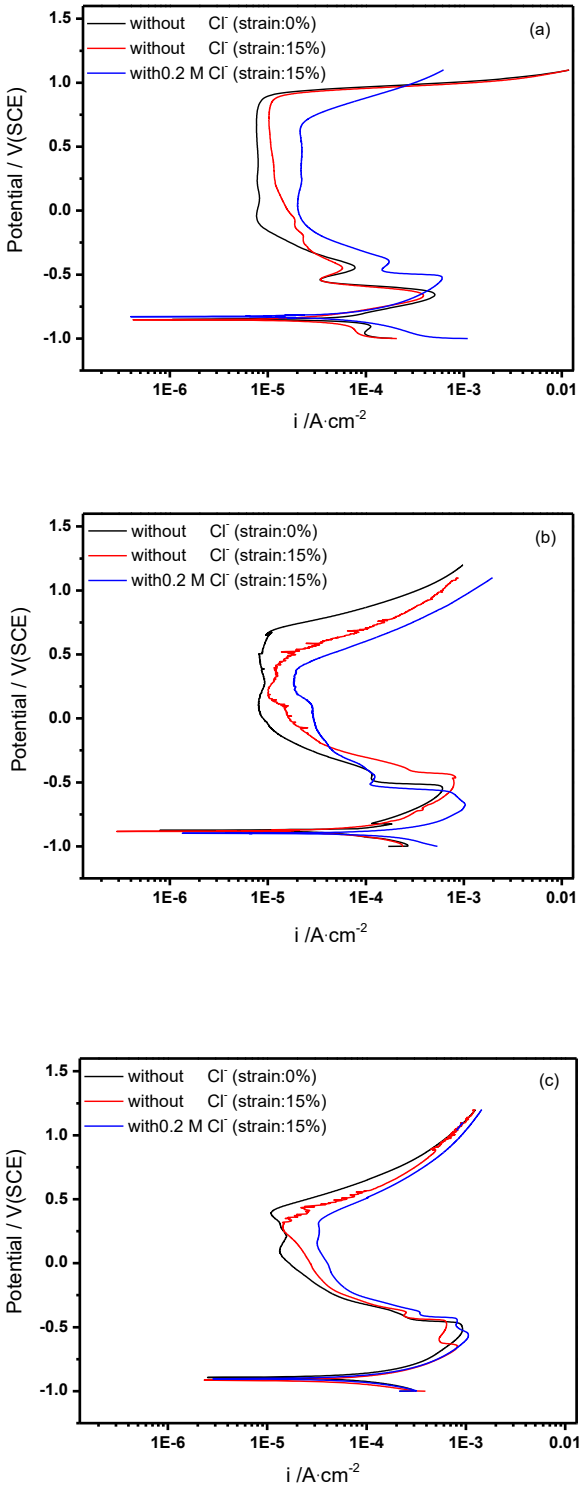

Figure 5. Polarization curves of X80 steel under the condition of some certain strain in 0.2M Cl^- containing alkaline solution at various AC current densities: (a) without AC, (b) 30A/m^2, (c) 50A/m^2

Table 1. Critical pitting potential (E_{br}/V) of X80 steel under different test condition

AC current density /A·m^{-2}	Without Cl^- (strain:0%)	Without Cl^- (strain:15%)	With 0.2M Cl^- (strain:15%)
0	0.883	0.874	0.661
30	0.683	0.442	0.377
50	0.399	0.367	0.318

Table 2. Passive current density (i_p/μA·cm^{-2}) of X80 steel under different test condition

AC current density /A·m^{-2}	Without Cl^- (strain:0%)	Without Cl^- (strain:15%)	With 0.2M Cl^- (strain:15%)
0	7.72	10.75	22.08
30	8.71	12.48	23.56
50	13.25	18.99	32.61

It may be that the existence of Cl^- further destroys the passive film, resulting in an increase in the amount of active points. In conclusion, the combined effect of AC interference, strain, and Cl^- causes a significant destructive impact on the passive film. Therefore, the three impact factors generate synergistic effect on the corrosion behavior of pipeline steel during the SCC process, resulting in an increase in the SCC susceptibility of the steel.

4. DISCUSSION

The above research results indicate that the addition of Cl^- increases the SCC susceptibility of X80 pipeline steels tested with or without AC application, but the mechanism is not changed. When AC current is not applied, the SCC mechanism of the steel in 0.2M Cl^- containing alkaline solution is anodic dissolution. In contrast, under AC application, the mechanism is attributed to the mixture of anodic dissolution with hydrogen embrittlement.

The previous research results [7] reported that the value of cathode current record via PS-12 potentiostat increases with the increased AC current density, and the negative current was -1.2 mA at an applied AC current density of 50 A/m^2. In this work, when Cl^- is added to the solution, the according negative current at 50 A/m^2 is higher, i.e. -1.8 mA. By comparison, the hydrogen evolution reaction of the steel electrode in Cl^- containing alkaline solution is more intense, and the larger amount of precipitated H atoms would ingress into the steel. Thus, the severity of hydrogen embrittlement of the steel further increases [24], and the SCC susceptibility is enhanced. Furthermore, the synergistic effect of AC and Cl^- [8] generates a more damage to the passive film, and pitting corrosion easily occurs on the steel surface. Thus, more cracks are initiated from the pitting, and it leads to the increase in the SCC susceptibility (Fig.3c-f). In addition, due to the occluded cell effect of crack tip, the chloride ion of the bulk solution can more easily migrate to the crack tip region, resulting in the enrichment of Cl^- [25] and the obvious effect of autocatalytic acidification. Then, the produced H atoms due to solution

acidification can diffuse toward the crack tip, which accelerates the anodic dissolution of the crack tip. Consequently, the addition of Cl^- improves the susceptibility of X80 pipeline steel to SCC.

Moreover, as it is seen from Fig.5 that, the synergistic effect of AC, strain, and Cl^- severely degrades the passivity of the steel, which facilitates the SCC behavior and further increases the SCC susceptibility.

5. CONCLUSIONS

AC and Cl^- generate the synergistic effect, causing an increase in the SCC susceptibility of X80 pipeline steel. And the fracture surface shows significant feature of brittle fracture. The addition of Cl^- increases the SCC susceptibility of steels with or without AC application, but the mechanism is not changed. At the absence of AC current, the SCC mechanism of the steel in 0.2M Cl^- containing alkaline solution is anodic dissolution. In contrast, under AC application, the mechanism is attributed to the combination of anodic dissolution with hydrogen embrittlement.

ACKNOWLEDGEMENTS
This work was support by the National Natural Science Foundation of China (No. 51501164), the Natural Science Foundation of Zhejiang province (No. LY18E010004), the Project Funded by China Postdoctoral Science Foundation (No.2017M621974), and the National R&D Infrastructure and Facility Development Program of China (No. 2005DKA10400).

References

1. M.M. EI-Naggar, *Appl. Surf. Sci.,* 252(2006)6179.
2. A.Q. Fu and Y.F. Cheng, *Corros. Sci.,* 52(2010)612.
3. P. Linhardt and G. Ball, AC Corrosion: Results from Laboratory Investigations and from a Failure Analysis, CORROSION 2006, Houston, America, 2006, 160.
4. Y.B. Guo, H.Tan, D.G. Wang and T. Meng, *Anti-Corros. Method.M.,* 64(2017)599.
5. Z.L. Li and Y. Yang, *Acta Petro. Sin.,* 33(2012)164.
6. M. Zhu, C.W. Du, X.G. Li, Z.Y. Liu, S.R. Wang, J.K. Li and D.W. Zhang, *Electrochim. Acta*, 117(2014) 351.
7. M. Zhu, C.W. Du, X.G. Li, Z.Y. Liu, H. Li and D.W. Zhang, *Corros. Sci.,* 87(2014)224.
8. M. Zhu, C.W. Du, X.G. Li and Z.Y. Liu, *Mater. Corros.,* 66(2015)494.
9. A. Eslami, R. Kania, B. Worthingham, G.V. Boven, R. Eadie and W. Chen, *Corros. Sci.,* 53(2011) 2318.
10. R.N. Parkins, *Corrosion*, 52(1996)363.
11. GB/T 15970, Chinese National Standard for Stress Corrosion Cracking Tests, 2007.
12. Z. F. Wang and A. Atrens, *Metall. Mater. Trans. A*, 27(1996)2686.
13. Y.W. Kang, W.X. Chen, R. Kania, G.V. Boven and R. Worthingham, *Corros. Sci.,* 53(2011)968.
14. B.T. Lu, J.L. Luo and P.R. Norton, *Corros. Sci.,* 52(2010)1787.
15. G.A. Zhang and Y.F. Cheng, *Corros. Sci.,* 52(2010)960.
16. A. Mustapha, E.A. Charles and D. Hardie, *Corros. Sci.,* 54(2012)5.
17. A.A. Oskuie, T. Shahrabi, A. Shahriari and E. Saebnoori, *Corros. Sci.,* 61(2012)111.
18. M.A. Aran and J.A Szpunar, *Mater. Sci. Eng., A*, 528(2011)4927.

19. M.C. Li and Y.F. Cheng, *Electrochim. Acta*, 53(2008)2831.
20. M.C. Li and Y.F. Cheng, *Electrochim. Acta*, 52(2007)8111.
21. R.N. Parkins, W.K. Blanchard Jr and B.S. Delanty, *Corrosion*, 50(1994)394.
22. LW.Wang, L.J. Cheng, J.R. Li, Z.F. Zhu, S.W. Bai and Z.Y. Cui, *Materials*, 11(2018)465.
23. H.X. Wan, D.D. Song, Z.Y. Liu, C.W. Du, Z.P. Zeng, X.J. Yang and X.G. Li, *J.Nat. Gas Sci. Eng.*, 38(2017)458.
24. B. Gu, J. Luo and X. Mao,*Corrosion*, 55(1999)96.
25. G.C. LÜ, C.C. Xu, Y.M. LÜ and H.D. Cheng, *Chin.J.Chem.Eng.,* 16(2008)646.